Physicochem. Probl. Miner. Process., 58(1), 2021, 101-112

http://www.journalssystem.com/ppmp

Physicochemical Problems of Mineral Processing

ISSN 1643-1049

Received August 06, 2021; reviewed; accepted December 01, 2021

Understanding the collection behavior of gangue minerals in fine flake graphite flotation

Wenlu Xu[1], Kangkang Sun[2], Yangshuai Qiu[1,3], Lingyan Zhang[1], Luo Yang[1], Shaowei Wei[1], Dafa Ding[1]

[1] School of Resources and Environmental Engineering, Wuhan University of Technology, Wuhan 430070, China

[2] School of Chemical Engineering, The University of Queensland, Brisbane, Queensland 4072, Australia

[3] Hubei Key Laboratory of Mineral Resources Processing & Environment, Wuhan 430070, China

Corresponding author: qiuyangshuai@whut.edu.cn (Y. Qiu)

Abstract: Flotation is one of the most common and effective methods for the beneficiation of natural graphite resources. However, the upgrading efficiency of flotation is always finite due to the undesirable collection of gangue minerals. In this work, the collecting mechanism of three typical gangue minerals, including mica, quartz, and feldspar, in fine flake graphite flotation was investigated. Results of batch flotation tests for single-minerals and artificial mixtures confirmed the enhanced collection of gangues in the presence of graphite particles. Contact angle and zeta potential results and theoretical calculations of the interaction between graphite and gangue particles based on typical DLVO theory indicated that it is impossible to collect gangue minerals by true flotation or through heterocoagulation with graphite particles. The fitting results of accumulated gangue recoveries and accumulated water recoveries using the Warren method demonstrated that most gangue minerals entered the concentrate through entrainment, with a small proportion by bubble inclusions.

Keywords: flake graphite, mica, quartz, flotation, entrainment

1. Introduction

Natural graphite, an important non-metallic mineral resource, is typically found in three commercial varieties: crystalline flake, microcrystalline or amorphous, and crystalline vein or lump (Chelgani et al., 2016; Peng et al., 2017; Sun et al., 2017; Qiu et al., 2016). Flake graphite can be divided into large flakes and fine flakes according to the size fraction. The peculiar physical and chemical properties of graphite such as high-temperature resistance, corrosion resistance, self-lubricating, electrical and thermal conductivity (Sure et al., 2012; Hu et al., 2014; Okada et al., 2017; Chen et al., 2018) make it very promising in various scientific and technical fields, including metallurgy, electronics, national defense, and aerospace. The rapid development of high-tech and advanced material-related industries in this new millennia has propelled the increasing demand for high quality and purity graphite resources; thus, those large flake graphite showing superior performance are more appreciated (Cermak et al., 2018).

Given the inherent hydrophobicity of graphite, froth flotation is perhaps the most effective and prevailing method for the initial upgrade of natural graphite minerals (Oney and Samanli, 2016). In flotation, hydrophobic graphite particles are selectively captured by air bubbles in the suspensions and transported towards the surface, leaving the hydrophilic gangue minerals, such as quartz, mica, and feldspar, in the suspension and being discharged as tailings. However, the upgrading efficiency of flotation is finite, and the final grade of the graphite is usually confined to 92-97% for large flake graphite (Wakamatsu and Numata, 1991; Peng et al., 2017), which is decent but still cannot meet the threshold of high-end utilization. Therefore, further purification with chemical treatment is always required. With the increasing consumption and depletion of large flake graphite resources, the exploration and

DOI: 10.37190/ppmp/144408

utilization of fine flake graphite ore have naturally received more attention (Jara et al., 2019).

However, many have observed that the smaller the graphite particles (or flake size), the lower grade of the final product by flotation (Bu et al.,2018; Bu et al., 2018; Jin et al., 2018). It is reported that besides true flotation, target minerals and gangues can sometimes enter the concentration through foam entrainment and bubble inclusion. Such entrainment and inclusion would become more noticeable in a denser suspension system with finer particles (Wang et al., 2015; Wang et al., 2016; Heyes and Trahar, 1977; Miettinen et al., 2010). Unlike true flotation, in which hydrophobic particles adhere to the surface of air bubbles, the entrainment is an unwanted process where the mineral particles, even hydrophilic, are entrapped in the water phase between the liquid films and mechanically transported upward as the foam rises. Foam inclusion refers to the phenomenon that the hydrophilic gangue mineral particles are sandwiched between the hydrophobic mineral particles that cannot be discharged. Therefore, they are carried into the concentrated foam with the target particles (Wang and Peng, 2013).

DLVO theory is commonly used to predict the favorable or unfavorable conditions for the bubble-particle interactions as well as particle-particle interactions (Gomez-Flores et al., 2020). To date, only a few studies (Li et al., 2014; Li et al., 2015; Weng et al., 2017; Yangshuai et al., 2019) have applied DLVO theory to reveal the interactions among different species in graphite flotation solution, and some of these studies have laterally indicated the presence of entrainment behavior in fine flake graphite flotation. For example, Li et al. (Li et al.,2015) found that sericite entered the foam through entrainment and inclusion in graphite flotation, verified by contact angle measurement and the Warren technique. However, the classical DLVO theory consisting of only the attractive Van der Waals energy and repulsive electrostatic double-layer interaction energy has been insufficient to predict the actual surface interactions. Some surface forces such as hydrophobic force are considered critical in understanding the aggregation and dispersion among particles, especially for those hydrophobic particles. Besides, other factors such as the surface roughness of the particles are also contributing (Yoon and Mao, 1996; Gomez-Flores et al., 2020). Our previous study (Yangshuai et al., 2017) on the interaction between fine flake graphite particles indicated that the aggregation of hydrophobic graphite particles is in better agreement with the XDLVO theory incorporating the hydrophobic interaction rather than the classical DLVO theory. Despite the previous studies regarding microcrystalline graphite and the interactions between fine flake graphite particles, the interactions between fine flake graphite and other gangue minerals have not been studied yet. Inspired by this, in this study, the collection mechanism of three gangue minerals (mica, quartz, and feldspar) in fine flake graphite flotation was studied via single-mineral and artificial mixture flotation tests. And the interactions between graphite and these gangues were calculated using the DLVO theory.

2. Experimental

2.1. Materials

The graphite, mica, quartz, and feldspar single-mineral samples were obtained from Yichang (Hubei, China), Xianning (Hubei, China), Xiushui (Jiangxi, China), and Feicheng (Shandong, China), respectively. All the samples were ground via ball milling using zirconia as the grinding medium and were subject to wet sieving and sedimentation classification to collect the -2 mm size fraction products for study. The samples were then purified with 10% hydrochloric acid for 0.5 h and washed with deionized water repeatedly before drying at 50℃ in a vacuum oven. X-ray diffraction (XRD) and X-ray fluorescence (XRF) analyses were applied to determine the mineralogical and chemical compositions of the samples, and the results are shown in Fig. 1 and Table. 1, respectively. As analyzed, the purities of gangue samples (mica, quartz, and feldspar) were all above 90 wt%. Note that the fixed carbon (FC) of graphite single-mineral was analyzed using the Chinese standard GB/T3521-2008, assaying 95.75 wt% FC. Particle size distributions of test samples were determined by a BT-9300S laser particle size analyzer, and the results are seen in Table 2 and Fig. 2.

Kerosene, the collector, was purchased from Kermel Chemical Reagent Co., Ltd. (Kermel, Tianjin, China), and the frother sec-octanol ($C_8H_{18}O$) was purchased from Shanghai Aladdin Biochemical Technology Co., Ltd (China). HCl and NaOH using as the pH regulators were purchased from Dongguan Yuantao Chemical Co., Ltd (China). All chemicals were of analytical grade and used directly without further purification. Deionized water (resistivity of 18.25 MΩ·cm) was used in this work.

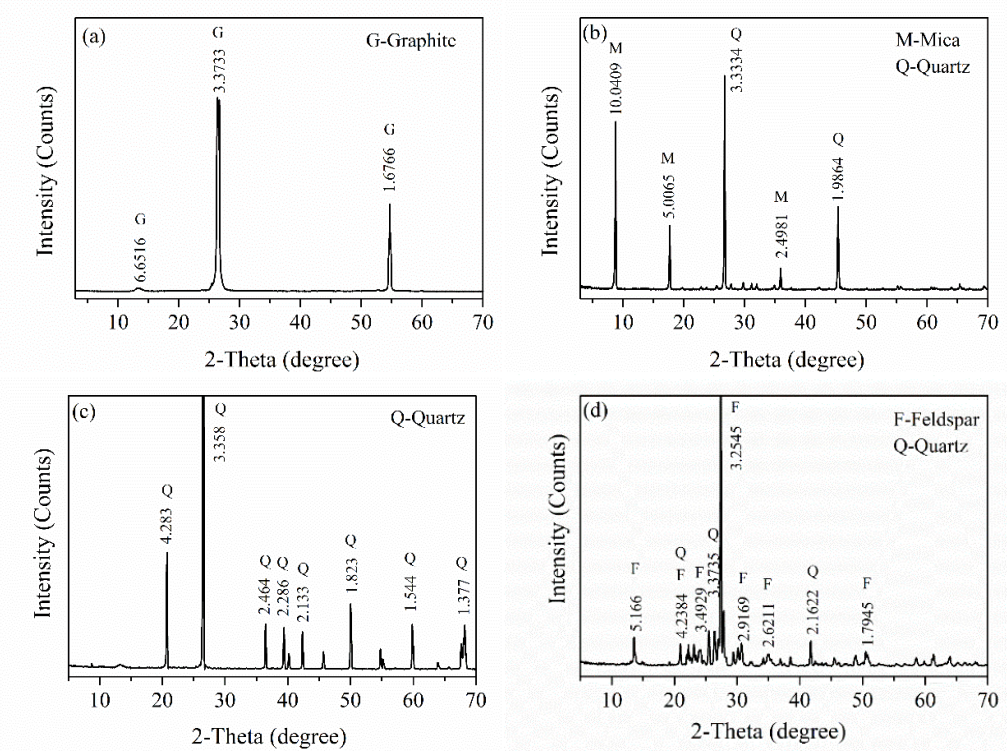

Fig. 1. X-ray diffraction (XRD) patterns of the single mineral samples: (a) graphite; (b) mica; (c) quartz; (d) feldspar

Table 1. Chemical compositions of mica, quartz, and feldspar single minerals (wt %)

Minerals	SiO_2	Al_2O_3	Fe_2O_3	CaO	K_2O	Na_2O	SO_3	MgO	Other
Mica	48.51	37.04	0.48	0.05	9.17	1.09	0.09	0.17	3.71
Quartz	98.87	0.25	0.10	0.04	0.28	/	0.04	/	0.42
Feldspar	68.32	15.49	0.13	0.05	13.72	0.86	0.09	0.17	1.17

Table 2. Particle size distribution of single minerals

Single mineral	D10 (μm)	D50 (μm)	D90 (μm)	Average diameter (μm)
graphite	39.17	66.60	110.10	60.77
mica	26.69	63.84	128.30	47.35
quartza	27.29	60.94	123.30	46.59
feldspar	25.52	62.02	128.70	45.45

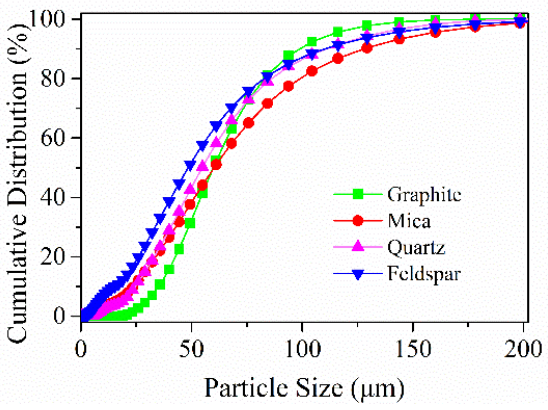

Fig. 2. Particle size distribution of single minerals

2.2. Batch flotation tests

The batch flotation tests of single minerals and artificial mixtures were conducted using an RK/FGC5-35 flotation cell (volume = 140 mL). The flotation slurry was first prepared by adding 2 g graphite or gangue particles (-74 μm size) to 100 mL of solution for single flotation or 2.5 g of the artificial mixture (2 g graphite and 0.5 g gangue) for mixed flotation. The experiment was carried out under neutral pH condition. The solution was conditioned for 3 min with an agitation speed of 1400 rpm to ensure complete dispersion of the particles. Then, the desired amount of collector kerosene and a fixed 20 mg/L of frother sec-octanol were added to the pulp and conditioned at a time sequence of 3 min. The flotation was then performed for another 3 min. Finally, collecting and calculating the mass fractions of floated and un-floated products yields the flotation recovery.

2.3. Zeta potential measurements

Zeta potential analysis of the samples (-3 μm) was determined using a Malvern Zetasizer Nano ZS90 (the UK) equipped with a rectangular electrophoresis cell. Specifically, the sample was first put into deionized water and stirred for 3 min. Then, the upper suspension was picked and injected into the cell for testing.The desired neutral pH 7 of the suspension was adjusted by dilute HCl or NaOH aqueous solutions. All the tests were conducted at room temperature of 25°C.

2.4. Contact angle measurements

The Washburn method was used to determine the contact angle of samples, as demonstrated in Fig. 2. First, a certain amount of solid sample power (-74 μm) was put into a sample tube with an inner diameter of 1.5 cm. The tube bottom was sealed with a microplate. The sample-contained tube was then immersed in the liquid of known surface tension. Driven by the capillary force, a rise of liquid can be expected. It is essential to fix the tube position and record the liquid uprising heights (h) as a function of time. Each sample was repeated at least three times, and all experiments were carried out at a room temperature of 25°C.

The Washburn equation (Guancheng, 2018) (Eq. (1)) was then used to calculate the contact angle of the sample:

$$h^2 = \frac{\gamma R cos\theta}{2\eta} \times t \tag{1}$$

where γ is the surface tension of the liquid, R is the effective capillary radius, η is the viscosity of the liquid, θ is the contact angle, and t is the time.

Note that there are two unknown terms, R and $cos\theta$, in this equation. The R can be determined using several low-energy apolar liquids such as heptane, octane, and dodecane. For the complete spreading of these liquids, $cos\theta = 1$ and R can thus be derived from the equation.

2.5. Interactions between graphite and gangues

DLVO theory was used to calculate the agglomeration and dispersion behaviors between graphite and gangue particles. The interaction forces, including Van der Waals energy (U_A), electrostatic double-layer interaction energy (U_R), and the total interaction energy (U_T), are described in Eqs. (2-5), respectively (Adair et al., 2001; Hamaker, 1937; Yangshuai et al., 2017; Mitchell et al., 2005):

$$U_A = \frac{A_{123} R_1 R_2}{6H(R_1+R_2)} \tag{2}$$

where the average radius of graphite particle R_1 was 30.38 μm (Table 2), the average radius of mica, quartz, and feldspar particle R_2 was 23.67 μm, 23.2 μm, and 22.77 μm, respectively (Table 2); H is the inter-surface separation distance between the particles. A_{132} is the Hamaker constant for the two different particles interacting through liquid medium 3, approximated from Eq. (3):

$$A_{132} \approx \left(\sqrt{A_{11}} - \sqrt{A_{33}}\right)\left(\sqrt{A_{22}} - \sqrt{A_{33}}\right) \tag{3}$$

where A_{11}, A_{22}, and A_{33} are the Hamaker constants of particles 1 and 2 and the medium in vacuum, respectively. Here, the Hamaker constants of graphite, mica, quartz, and feldspar in vacuum are 23.8 × 10^{-20} J (Maurer et al., 2001), 9.86 × 10^{-20} J (Bergström, 1997), 5×10^{-20} J (Farahat, 2009), and 8.6 × 10^{-20} J,

respectively. When medium 3 is water (A_{33} = 3.7×10^{-20} J) (Yangshuai et al., 2017), a value of the Hamaker constant of 3.59 × 10^{-20} J was calculated for the mica/water/graphite system on the basis of Eq. 3; a value of the Hamaker constant of 9.00 × 10^{-21} J was calculated for the quartz/water/graphite system, and a value of the Hamaker constant of 2.98 × 10^{-20} J was calculated for the feldspar/water/graphite system.

$$U_R = \frac{\pi\varepsilon_0\varepsilon_1 R_1 R_2}{(R_1+R_2)}(\varphi_1{}^2 + \varphi_2{}^2)\left\{\frac{2\varphi_1\varphi_2}{\varphi_1{}^2+\varphi_2{}^2} ln\left[\frac{1+e^{-\kappa H}}{1-e^{-\kappa H}}\right] + \ln(1-e^{-2\kappa H})\right\} \quad (4)$$

where φ_1 and φ_2 are the zeta potentials of the particle surface, ε_0 is the vacuum permittivity (8.854 × 10^{-19} C^2/J/m), ε_r is the relative permittivity of the medium water (78.5 for pure water), and κ is the reciprocal of the Debye constant (κ = 0.10 nm^{-1}); that is, $1/\kappa$ is the Debye length, also referring to the electrical double layer thickness (Wan, 1997; Israelachvili, 1992). The energy was normalized to kT units in this study (Note that kT=4.11 × 10^{-21} J at the temperature of 298K).

$$U_T = U_A + U_R \quad (5)$$

2.6. Determination of entrainment and true flotation

The Warren method (Warren, 1985) was applied to understand the recycling mechanisms of hydrophilic gangue minerals in graphite flotation. Specifically, Warren proposed that the recovery of gangue particles is attributed to the summation of true flotation and entrainment, as described in Eq. (6):

$$R_G = F + R_E = F + e \times R_w \quad (6)$$

where R_G is the total recovery of gangue, F is the true flotation recovery of gangue, R_E is the entrainment recovery of gangue, R_W is the water recovery of the froth product (calculated using Eq. (7)), and e is the entrainment rate of gangue.

$$R_w = \frac{M_1 - M_2}{M_w} \quad (6)$$

where M_1 and M_2 are the wet weight and dry weight of the froth product, respectively (%), M_w is the weight of water consumed during the flotation process (%).

A series of accumulated recoveries of gangue $R^c_G(t)$ and accumulated water recoveries $R^c_W(t)$ at a given time was calculated as a function of the flotation time with certain foam phase thickness. Subsequently, the F and e can be determined via the linear fitting of the series of $R^c_G(t)$ and $R^c_W(t)$ using Eq. (6). In detail, three different froth thicknesses were selected, and the collection of froth products was carried out at multiple periods: 0~0.25 min, 0.25~0.5 min, 0.5~1 min, 1~1.5 min, 1.5~2 min, 2~3 min, and 3~4 min, respectively.

3. Results and discussion

3.1. Flotation and wetting results

Fig. 3a shows the flotation recoveries of graphite and gangue single-mineral particles as a function of collector kerosene dosage. As a naturally floatable mineral, a decent flotation recovery (above 70%) of graphite is witnessed even in the absence of collector kerosene. With the increase of kerosene dosage, the floatability of graphite is enhanced, and the recoveries reach nearly 100% when the kerosene dosage exceeds 80 mg/L. In contrast, the flotation recoveries of gangue minerals (mica, quartz, and feldspar) are less than 10% over the whole kerosene dosage range, and more interestingly, show a slight decrease trend with the increase of collector concentration. In theory, efficient flotation separation of gangue minerals and flake graphite can be expected. However, the intriguing flotation phenomena of artificially mixed minerals, as shown in Fig. 3b, have challenged this estimation. In detail, graphite recoveries in mixed flotation show a similar upward trend and can be fully collected, similar to the single-mineral flotation. By contrast, the collection efficiencies of mica, quartz, and feldspar all experience significant enhancement, with the recoveries increasing from an initial 10% in the absence of kerosene to around 25-30% at a high kerosene dosage of 250 mg/L.

It is generally accepted that the discrepancy in surface hydrophobicity between different minerals is a prerequisite for their flotation separation. These hydrophilic materials are wetted and soaked into water, while hydrophobic materials remained at the interface. Therefore, the hydrophobicity of these minerals was determined using contact angle measurement, and the results are shown in Fig. 4. The contact angle of graphite is 60.13° without kerosene addition, which verifies the strong hydrophobicity

of natural flake graphite minerals. And the increased contact angle at higher kerosene concentration is well consistent with the enhanced floatability, as shown in Fig. 3a. By contrast, the contact angles of mica, quartz, and feldspar are 20°, 14°, and 10°, respectively, in the absence of kerosene, demonstrating distinct hydrophilic properties of these gangues. Moreover, there is an indiscernible change of contact angles with the increase of kerosene concentration, which means that the presence of kerosene does not affect the surface properties of gangue minerals, corresponding to their negative flotation responses (Fig. 3a). Therefore, the significant increasing recoveries of gangue minerals in the mixed flotation must not be caused by the surface hydrophobicity change of these gangues but by other factors. More obviously, there is a similar flotation recovery trend between graphite and gangues when mixed; thus, it is not unreasonable to assume that the collection of gangue minerals is more likely affected by the graphite particles rather than by true flotation.

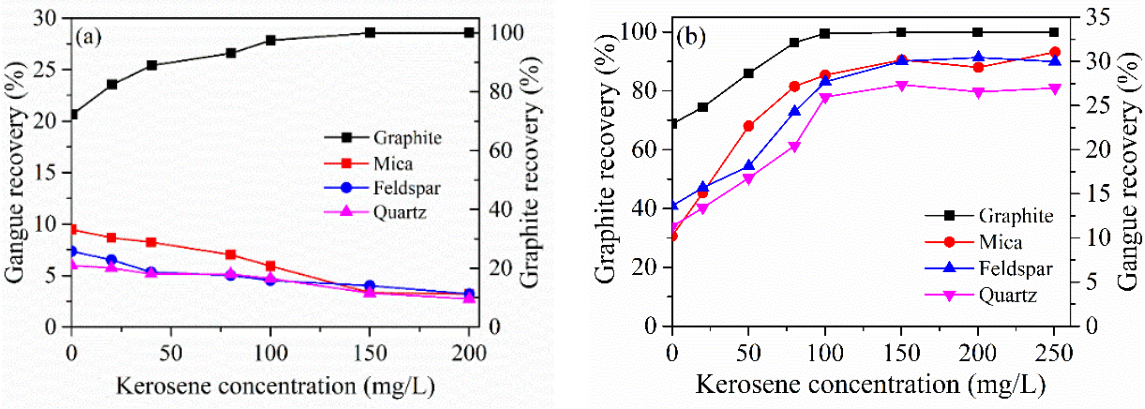

Fig. 3. Effect of kerosene dosage on the flotation recovery of graphite and gangue minerals: (a) single mineral flotation and (b) artificial mixture flotation in the presence 20 mg/L of frother sec-octanol at pH=7

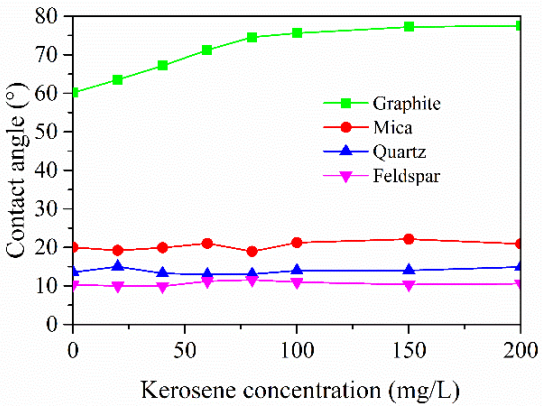

Fig. 4. Effect of kerosene dosage on the contact angle of graphite and gangue minerals

3.2. Surface potential and interactions between graphite and gangue

Since the gangue minerals were not collected via hydrophobization by collectors, some interactions between graphite and gangue minerals, such as heterocoagulation or surface cover, might contribute to the collection of gangue minerals. Inspired by this, the coagulation and dispersion behaviors between graphite and gangues were investigated via the measurement of surface potential and the force calculation using the DLVO theory. The zeta potential is a helpful factor in characterizing the stability of colloidal dispersions and providing vital information for the measurement of interaction forces between associated particles. By zeta potential measurement, the zeta potentials of graphite, mica, quartz, and feldspar at neutral pH 7 are -17.1 mV, -47.3 mV, -41.7 mV and -39.4 mV, respectively. Thus, these particles are more prone to stay dispersed in the solution due to the electrostatic repulsion between similar negatively charged surfaces.

Quantitatively, the total interaction energy U_T between graphite and gangue mica , quartz or feldspar

at neutral pH condition was calculated by Eqs. (2-5), and the results are given in Fig. 5. As shown, the maximum U_T between graphite and mica particles is 4588.25 kT at a distance of 7.4 nm. Consequently, the repulsion energy of 4588.25 kT must be overcome to form the aggregates of graphite and mica. Similarly, when the distance between graphite and quartz particles is 4.6 nm, the maximum total interaction energy U_T between graphite and quartz particles is 6513.57 kT. When the distance between graphite and feldspar particles is 6.4 nm, the maximum total interaction energy U_T between graphite and quartz particles is 4260.47 kT. However, it is difficult for graphite and mica mica , quartz or fledspar to overcome such high energy barriers and form the aggregates. Therefore, it is unlikely that mica and quartz can enter the graphite concentrate by forming aggregates with graphite particles. Similar observation has been reported by other researchers (Li et al., 2015; Yu et al.2018).

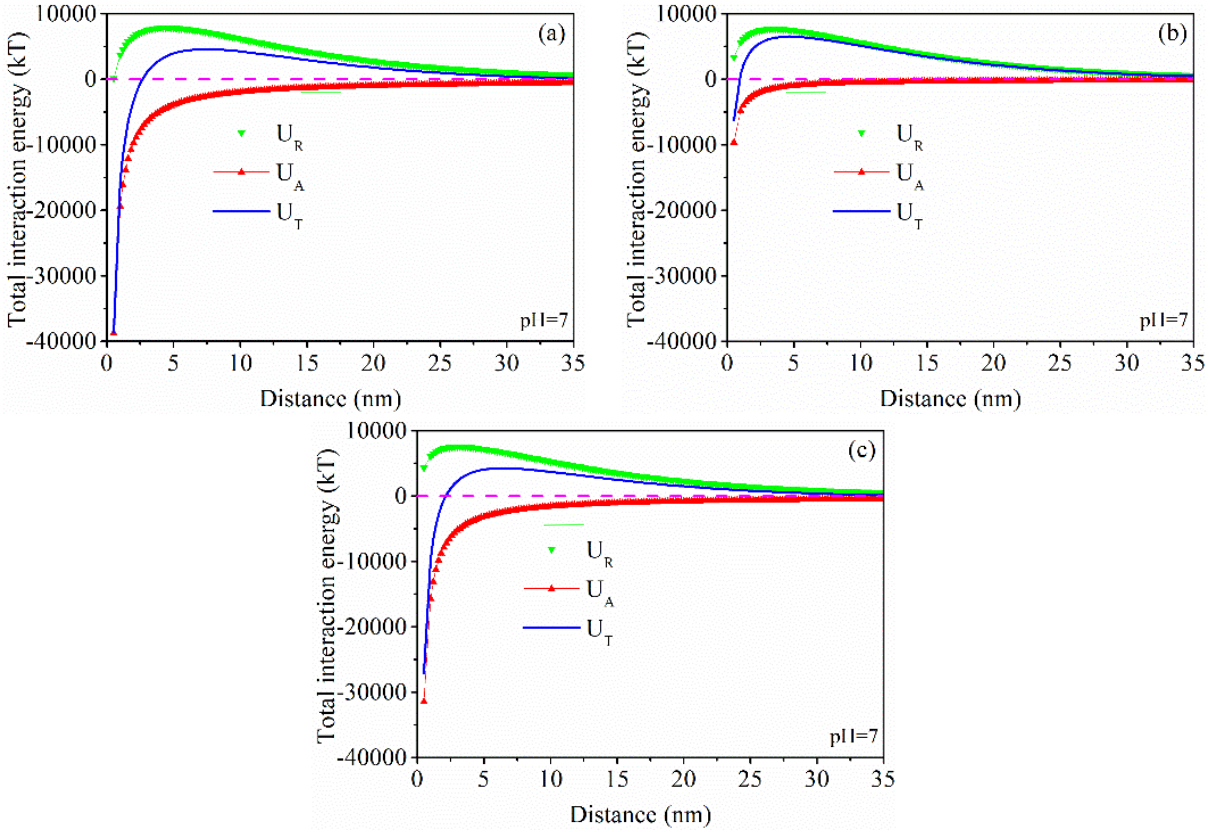

Fig. 5. Interaction potential energy between graphite and gangue minerals: (a) mica ; (b) quartz; and (c) feldspar at pH=7

3.3. True flotation volume and entrainment volume of gangue minerals

The previous results have denied the possibilities of gangue collection through true flotation and heterocoagulation with graphite particles. It is assumed that most gangue minerals enter the graphite concentration through entrainment and inclusion, given the condition of sufficient liberation. Here, the method proposed by Warren was applied to determine the proportion of gangue minerals entering the concentrate by entrainment and inclusion in fine flake graphite flotation. The foam layer thicknesses were controlled at 10 mm, 20 mm, and 30 mm, respectively, and the results are shown in Tables 3, 4, and 5.

From Tables. 3-5, the stage entrainment factor *e(t)* of gangue minerals gradually decreases with time, and the majority of water and target minerals are collected within 1.5 min. Therefore, it is appropriate to use the Warren method to determine the entrainment and true flotation of gangue minerals within this period and the fitting results of accumulated recoveries of gangue $R_G^c(t)$ and accumulated water recoveries $R_W^c(t)$ within 0-1.5 min are given in Fig. 6.

According to Warren's hypothesis, the recovery of mica, feldspar, and quartz by true flotation are no more than 1.71%, 1.55%, and 1.29% (the intercepts in Fig. 6), respectively, while the cumulative

recovery of mica, feldspar, and quartz are about 30%, 24%, and 23% (Fig. 3b), respectively. As a result, true flotation only accounts for less than 7% of the total recovery of gangue minerals in the mixed flotation, while more than 93% of them are collected by entrainment. Besides, even the 7% recovery was not necessarily contributed by true flotation. The low contact angles of mica, feldspar, and quartz after interacting with kerosene (only about 20°, 13°, and 10°, respectively), as shown in Fig. 4, are insufficient to ensure their collection through real flotation. For example, some (Zheng et al., 2006) assumed that inclusion might be another mechanism for the collection of siliceous gangue minerals if the entrainment factor was larger than 1. From Tables. 3-5, in the early stage of flotation, the stage entrainment factor *e(t)* of gangue minerals is greater than 1, which indicates that instead of true flotation, inclusion might partly contribute to the 7% recovery of mica, feldspar, and quartz. In addition, the thickness of the froth layer is another factor affecting particle inclusion. Generally, the thicker the froth layer, the thinner the liquid film between bubbles, and thus the greater chance of particle inclusion. Taking mica as an example, in the initial 0.25 min, the *e(t)* of mica is 1.03 when the thickness of the foam layer is 10 mm. As the thickness increases to 30 mm, the *e(t)* increases to 1.14; that is, with the increase of the thickness of the foam layer, the amount of gangue minerals entrained into the concentrate will also increase accordingly.

Table. 3 The effect of flotation time on the recoveries of water and mica and the entrainment factor in mixed flotation

Froth layer thickness /mm	Time /min	$R_w^c(t)$/%	$R_g^c(t)$/%	e(t)	$e^c(t)$
10	0-0.25	8.13	8.58	1.06	1.06
	0.25-0.5	17.36	17.53	1.01	0.97
	0.5-1	29.51	28.62	0.97	0.91
	1-1.5	33.47	30.46	0.91	0.46
	1.5-2	36.15	30.73	0.85	0.10
	2-3	37.88	31.06	0.82	0.19
	3-4	39.29	31.43	0.80	0.26
20	0-0.25	7.02	7.79	1.11	1.11
	0.25-0.5	15.83	15.51	0.98	0.88
	0.5-1	26.04	24.74	0.95	0.90
	1-1.5	31.58	28.42	0.90	0.66
	1.5-2	34.21	30.10	0.88	0.64
	2-3	36.77	31.25	0.85	0.45
	3-4	37.96	31.51	0.83	0.21
30	0-0.25	5.39	6.14	1.14	1.14
	0.25-0.5	11.69	11.81	1.01	0.90
	0.5-1	19.21	18.63	0.97	0.91
	1-1.5	28.64	26.35	0.92	0.82
	1.5-2	33.05	28.75	0.87	0.55
	2-3	35.42	29.04	0.82	0.12
	3-4	37.01	29.24	0.79	0.12

Table. 4 The effect of flotation time on the recoveries of water and feldspar and the entrainment factor in mixed flotation

Froth layer thickness /mm	Time /min	Rc w(t)/%	Rc g(t)/%	e(t)	ec(t)
10	0-0.25	6.53	6.40	0.98	0.98
	0.25-0.5	13.59	13.05	0.96	0.94
	0.5-1	20.48	18.43	0.90	0.78
	1-1.5	25.27	21.23	0.84	0.58
	1.5-2	27.02	22.16	0.82	0.53
	2-3	28.11	22.49	0.80	0.30
	3-4	29.14	22.73	0.78	0.23
20	0-0.25	6.02	6.14	1.02	1.02
	0.25-0.5	12.98	12.85	0.99	0.96
	0.5-1	18.39	16.92	0.92	0.75
	1-1.5	24.12	20.74	0.86	0.67
	1.5-2	28.64	24.06	0.84	0.73
	2-3	29.58	24.26	0.82	0.21
	3-4	30.79	24.32	0.79	0.06
30	0-0.25	4.98	5.13	1.03	1.03
	0.25-0.5	10.98	10.76	0.98	0.94
	0.5-1	17.85	16.24	0.91	0.80
	1-1.5	25.13	22.11	0.88	0.81
	1.5-2	29.36	24.96	0.85	0.67
	2-3	30.21	25.07	0.83	0.14
	3-4	31.44	25.15	0.80	0.06

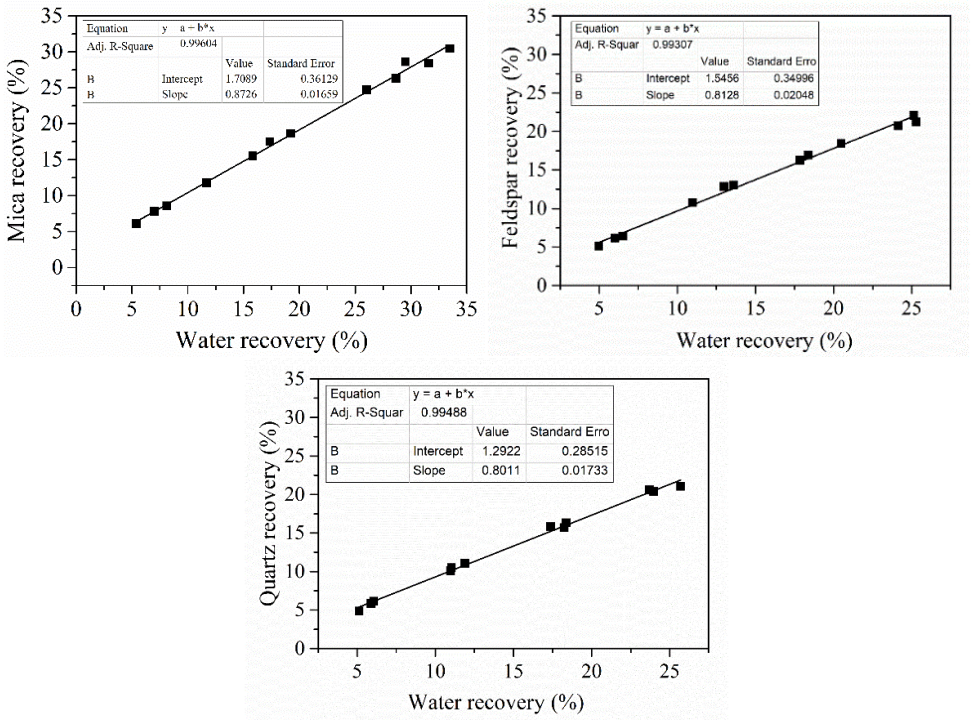

Fig. 6. The Warren method for the determination of entrainment and true flotation in mixed mineral flotation: (a) mica, (b) feldspar, and (c) quartz

Table. 5 The effect of flotation time on the recoveries of water and quartz and the entrainment factor in mixed flotation

Froth layer thickness /mm	Time /min	Rc w(t)/%	Rc g(t)/%	e(t)	ec(t)
10	0-0.25	5.12	4.86	0.95	0.95
	0.25-0.5	10.98	10.10	0.92	0.89
	0.5-1	18.25	15.70	0.86	0.77
	1-1.5	25.69	21.07	0.82	0.72
	1.5-2	29.41	22.94	0.78	0.50
	2-3	31.23	23.11	0.74	0.09
	3-4	32.05	23.40	0.73	0.35
20	0-0.25	5.89	5.83	0.99	0.99
	0.25-0.5	11.88	11.05	0.93	0.87
	0.5-1	18.36	16.34	0.89	0.82
	1-1.5	23.97	20.37	0.85	0.72
	1.5-2	28.12	22.50	0.80	0.51
	2-3	29.47	22.99	0.78	0.36
	3-4	30.25	23.29	0.77	0.39
30	0-0.25	6.07	6.13	1.01	1.01
	0.25-0.5	11.04	10.49	0.95	0.88
	0.5-1	17.39	15.82	0.91	0.84
	1-1.5	23.69	20.61	0.87	0.76
	1.5-2	28.77	23.88	0.83	0.64
	2-3	29.99	23.99	0.80	0.09
	3-4	30.97	24.16	0.78	0.17

4. Conclusions

In this work, the flotation behaviors of graphite and the main co-existing gangue minerals, including mica, quartz, and feldspar, have been studied through both single-mineral flotation and artificial mixed-mineral flotation tests. The results showed that these gangue minerals were barely floatable in their single-mineral flotation systems. However, a substantial flotation recovery increase of these gangues was obtained once mixed with graphite particles. Specifically, less than 10% of gangue particles were collected in their single flotation, while the maximum recovery of gangue exceeded 30% in the mixed flotation.

Such intriguing discrepancy between single and mixed flotation has been further studied by contact angle measurement, zeta potential measurement, and the Warren method. The limited contact angles of gangue minerals over the whole collector concentration range have denied the possibility of true flotation of these gangues by hydrophobization. By calculating the interaction energy between graphite and gangue minerals using the DLVO theory, no heterocoagulation or slime coating occurred due to the unconquerable repulsion forces between them. The fitting results of accumulated recoveries of gangue and accumulated water recoveries using the Warren method demonstrated that approximately 93% of gangue minerals in the mixed flotation were collected through entrainment, and the rest were mainly through inclusion. Our results have provided substantial evidence on the entrainment phenomenon of gangue minerals, including mica, quartz, and feldspar, in the flotation separation of fine flake graphite resources. Therefore, further studies regarding the contributing factors on entrainment and how to minimize entrainment in flake graphite flotation are proposed to investigate in the future.

Acknowledgments

This research was supported by National key research and development plan(2020YFC1909604). The authors also gratefully acknowledge the assistance of National key research and development plan(2020YFC1909604).

References

ADAIR, J.H., SUVACI, E., SINDEL, J., 2001.*Surface and Colloid Chemistry. In: Buschow KHJ, Cahn RW, Flemings MC, Ilschner B, Kramer EJ, Mahajan S, et al., (editors).* Encyclopedia of Materials: Science and Technology. Oxford: Elsevier, p. 1-10.

BERGSTRÖM, L., 1997.*Hamaker constants of inorganic materials. Advances in Colloid and Interface Science.*70:125-69.

BU, X.N., ZHANG, T.T., CHEN, Y.R., PENG, Y.L., XIE, G.Y., WU, E.D., 2018.*Comparison of mechanical flotation cell and cyclonic microbubble flotation column in terms of separation performance for fine graphite.* Physicochemical Problems of Mineral Processing, 54, 732-40.

BU, X.N., ZHAGN, T.T., PENG, Y.L., XIE, G.Y., WU, E.D., 2018.*Multi-Stage Flotation for the Removal of Ash from Fine Graphite Using Mechanical and Centrifugal Forces.* Minerals. 8.

CHELGANI, S.C., RUDOLPH, M., KRATXSH, R., SANDMANN, D., GUTZMER, J., 2016. *A Review of Graphite Beneficiation Techniques.* Mineral Processing and Extractive Metallurgy Review. 37, 58-68.

CHEN, Z., LIU, Y., ZHANG, Y., SHEN, F., YANG, G., WANG, L., et al., 2018. *Ultrafine layered graphite as an anode material for lithium ion batteries.* Materials Letters, 229, 134-7.

CERMAK, M., BAHRAMI, M., KENNA, J.,2018. *Natural Graphite Sheet Heat Sinks: A Review of the Material Properties, Benefits, and Challenges.* PROCEEDINGS 2018 34TH ANNUAL SEMICONDUCTOR THERMAL MEASUREMENT, MODELLING & MANAGEMENT SYMPOSIUM (SEMI-THERM), p. 55-62.

FARAHAT, M., HIRAJIMA, T., SASAKI, K., DOI, K., 2009. *Adhesion of Escherichia coli onto quartz, hematite and corundum: Extended DLVO theory and flotation behavior.* Colloids and Surfaces B: Biointerfaces. 74, 140-9.

GOMEZ-FLORES, A., SOLONGO, SK., HEYES, GW., ILAYS, S., KIM, H., 2020. *Bubble - particle interactions with hydrodynamics, XDLVO theory, and surface roughness for flotation in an agitated tank using CFD simulation.* Minerals Engineering.152.

GUANCHAENG, J., 2018.*Chapter 2 - Evaluation Methods and Influencing Factors of Gas Wettability.* In: Guancheng J, (editor). Gas Wettability of Reservoir Rock Surfaces with Porous Media: Gulf Professional Publishing, p. 29-84.

HAMAKER, H.C., 1937. *The London – van der Waals attraction between spherical particles.* Physica. 4, 1058-72.

HEYES,G.W.,TRAHAR,W.J.,1977.*The natural flotability of chalcopyrite.* International Journal of Mineral Processing.317-344.

HU, Z.Q., WANG, Z.S., CHEN, J.G., FAN B.L., QI, X, MA J., GU, Y.Y., SONG, L., 2014. *Effects of Surface-Modified Graphite on Tribological Properties and Thermal Conductivity of Fabric Self-Lubricating Liner.* Asian Journal of Chemistry. 26, 5712-6.

ISRAELACHVILI,J.N., 1992. *Intermolecular and surface forces.* ACADEMIC PR.

JARA, A,D,, BETEMARIAM, A., WOLDETINSAE, G., KIM, J.Y., 2019.*Purification, application and current market trend of natural graphite: A review.* International Journal of Mining Science and Technology, 29, 671-89.

JIN, M., XIE, G., XIA, W., PENG, Y., 2018.*Flotation Optimization of Ultrafine Microcrystalline Graphite Using a Box-Behnken Design.* International Journal of Coal Preparation and Utilization, 38, 281-9.

LI, H.Q., FENG, Q.M., YANG, S.Y., OU, L.M., LU, Y., 2014. *The entrainment behaviour of sericite in microcrystalline graphite flotation.* International Journal of Mineral Processing, 127, 1-9.

LI, H.Q., OU, L.M., FENG, Q.M., CHANG, Z.Y., 2015. *Recovery mechanisms of sericite in microcrystalline graphite flotation.* Physicochemical Problems of Mineral Processing, 51, 387-400

MAURER,S., MERSMANN, A., PEUKERT,W., 2001. *Henry coefficients of adsorption predicted from solid Hamaker constants.* Chemical Engineering Science, 56, 3443-53.

MIETTINENA, T., RALXTONB,J., FORNASIERB, D.,2009. *The limits of fine particle flotation.* Minerals Engineering, 420-477.

MITCHELL, T.K., NGUYEN A.V., EVANS, G.M., 2005.*Heterocoagulation of chalcopyrite and pyrite minerals in flotation separation.* Advances in Colloid and Interface Science, 114-115, 227.

ROE-HOAN, Y,. LAIQUN, M,.1996. *Application of Extended DLVO Theory, IV.* Journal of colloid and interface science, 184(1), 613-626.

OKADA, M., OHTA, N., YOSHIMOTO, O., TATSUMI, M., INAGAKI, M., 2017.*Review on the high-temperature*

resistance of graphite in inert atmospheres. Carbon, 116, 737-43.

ONEY, O., SAMANLI, S., 2016. *Determination of optimal flotation conditions of low-grade graphite ore.* In: Kowalczuk PB, Drzymala J, (editors). Mineral Engineering Conference, 8..

PENG, W.J., WANG, C., HU, Y., SOMG S.X., 2017. *Effect of droplet size of the emulsified kerosene on the floatation of amorphous graphite.* Journal of Dispersion Science and Technology, 38, 889-94.

PENG, W.J., QIU, Y.S., ZHANG, L.Y., GUANG, J.F., SOMG, S.X.,2017. *Increasing the Fine Flaky Graphite Recovery in Flotation via a Combined MultipleTreatments Technique of Middlings,* Minerals.7.

QIU, Y.S., YU, Y.F., ZHANG, L.Y., QIAN, Y.P., OUYANG, Z.J., 2016. *An Investigation of Reverse Flotation Separation of Sericite from Graphite by Using a Surfactant: MF,* Minerals. 6.

SUN, K., QIU, Y., ZHANG, L.Y., 2017.*Preserving Flake Size in an African Flake Graphite Ore Beneficiation Using a Modified Grinding and Pre-Screening Process.* Minerals, 7, 115.

SURE, J., RAVI SHANKAR, A., RAMYA, S., KAMACHI MUDALI, U., 2012.*Molten salt corrosion of high density graphite and partially stabilized zirconia coated high density graphite in molten LiCl–KCl salt.* Ceramics International, 38, 2803-12.

WAKDMATSU, T., NUMATA, Y., 1991.*FLOTATION OF GRAPHITE.* Minerals Engineering, 4, 975-82.

WAN, Q.H., 1997. *Effect of Electrical Double-Layer Overlap on the Electroosmotic Flow in Packed-Capillary Columns.* Analytical Chemistry, 69, 361-3.

WANG, L., PENG, Y., RUNGE, K., BRADSHAW, D., 2015. *A review of entrainment: Mechanisms, contributing factors and modelling in flotation.* Minerals Engineering, 70, 77-91.

WANG, L., PENG, Y,, RUNGE, K., 2016. *Entrainment in froth flotation: The degree of entrainment and its contributing factors.* Powder Technology, 288, 202-11.

WANG, B., PENG, Y., 2013.*The behaviour of mineral matter in fine coal flotation using saline water. Fuel.* 109:309-15.

WARREN, L.J., 1985. *Determination of the contributions of true flotation and entrainment in batch flotation tests.* International Journal of Mineral Processing, 14, 33-44.

WENG, X.Q., LI, H.Q., SONG. S.X., LIU, Y.Y., 2017. *Reducing the Entrainment of Gangue Fines in Low Grade Microcrystalline Graphite Ore Flotation Using Multi-Stage Grinding-Flotation Process,* Minerals. 7.

YANGSHUAI, Q., ZHANG, L., SUN, K., LI, Y., YUPENG, Q., 2019. *Reducing entrainment of sericite in fine flaky graphite flotation using polyaluminum chloride.* Physicochemical Problems of Mineral Processing, 55, 1108-19.

YANGSHUAI, Q.,YOMGFU, Y., LINGYAN, Z., WEIJUN, P., YUPENG, Q., 2017. *Dispersion and agglomeration mechanism of flaky graphite particles in aqueous solution.* Journal of Dispersion Science and Technology, 38, 796-800.

YU,Y.X.,MA,L.Q.,XU,H.X.,SUN, Z.J.,ZHANG.Z.J, YE,G.C,.2018 *DLVO theoretical analyses between montmorillonite and fine coal under different pH and divalent cations.* Powder Technology, 330, 147-151.

ZHENG, X., JOHNSON, N.W., FRANZIDIS, J.P., 2006. *Modelling of entrainment in industrial flotation cells: Water recovery and degree of entrainment.* Minerals Engineering, 19, 1191-203.